[Supplementary material]

Ground-penetrating radar survey at Falerii Novi: a new approach to the study of Roman cities

Lieven Verdonck[1], Alessandro Launaro[2], Frank Vermeulen[1] & Martin Millett[2,*]

[1] *Department of Archaeology, Ghent University, Belgium*

[2] *Faculty of Classics, University of Cambridge, UK*

[*] *Author for correspondence (✉ mjm62@cam.ac.uk)*

Data acquisition

Table S1. Instruments used for data acquisition.

Instruments used for data acquisition	
Geophysical instruments	Sensors & Software Spidar GPR network
Instruments for acquisition of position data	▪ Leica GS15 real time kinematic (RTK) GNSS receiver (with RTK corrections from reference stations in the ItalPoS network); ▪ Leica TS15 robotic total station (TS)

Table S2. Data acquisition parameters.

Data acquisition parameter	**Value**	**Remark**
Total area (ha)	26.6	
Duration of survey (weeks)	15	In three seasons (2015-17)
GPR antenna centre frequency (MHz)	500	
Temporal sample interval (ns)	0.2	
Time window (ns)	80	
Transect spacing (m)	~0.0625	
Distance between readings along the transects (m)	0.05	
Overall positioning accuracy in in-line and cross-line direction (m)	~0.05	This is the sum of the accuracy of GNSS/TS measurements and the accuracy when following the predefined trajectory with the ATV.

Data processing

Table S3. GPR data processing flow.

GPR data processing flow
DC-shift correction
Airwave alignment
Time zero estimation
Amplitude scaling
Low-pass frequency filtering (cut-off frequency: 1 GHz)
Calculation of individual antenna coordinates from raw GNSS position data
Creation of horizontal slices by interpolating the data on a regular grid of 0.05m × 0.05m
Background removal
De-striping of time slices by equalizing the average value of each channel in a swath
Migration velocity analysis (resulting in a wave velocity decreasing from 0.097m/ns at a two-way travel time of 10ns, to 0.07m/ns at 35ns)
2D phase-shift migration
Time-to-depth conversion

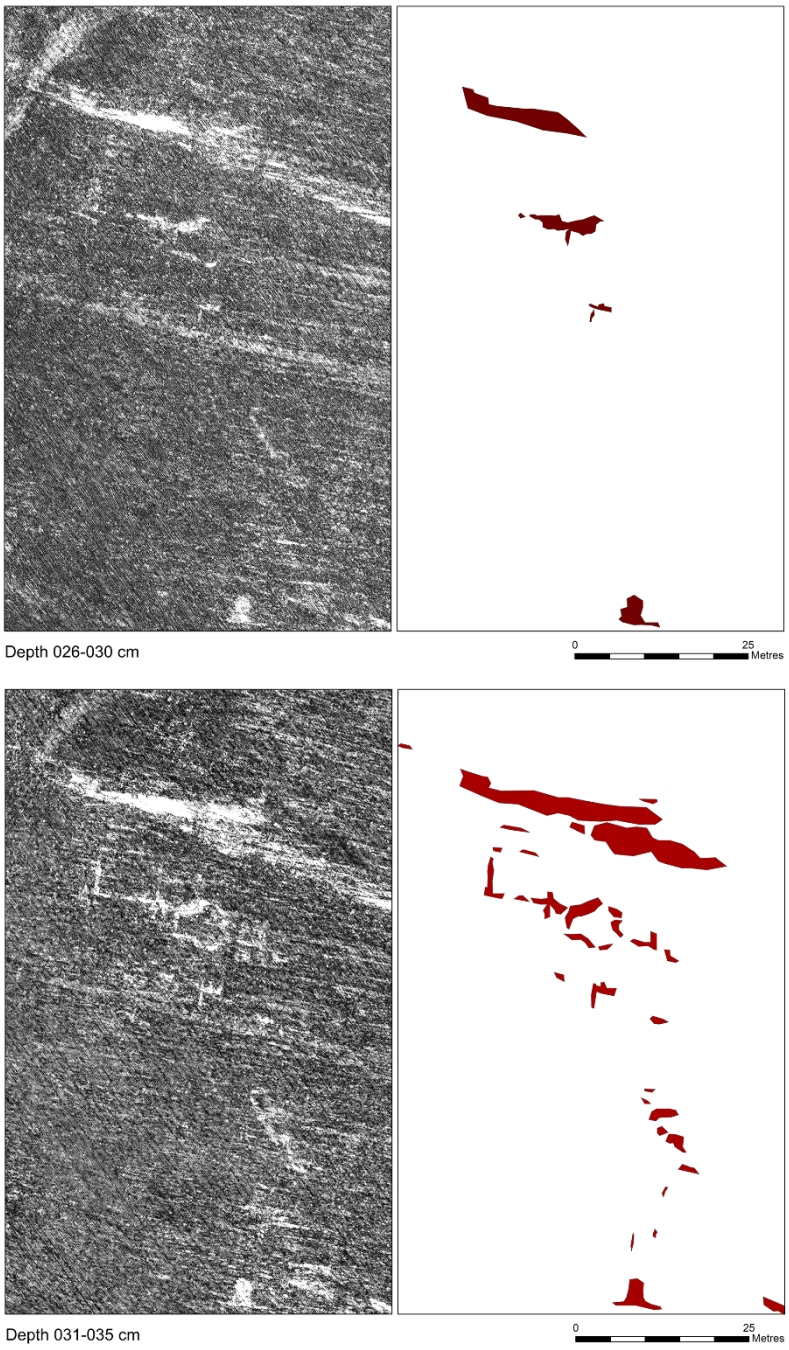

Figure S1. GPR time-slices from the sample area at Falerii Novi (for location see Figure 4) at depths 026–030cm and 031–035cm: left) GPR image; right) manually mapped anomalies (illustration: A. Launaro; GPR data: L. Verdonck).

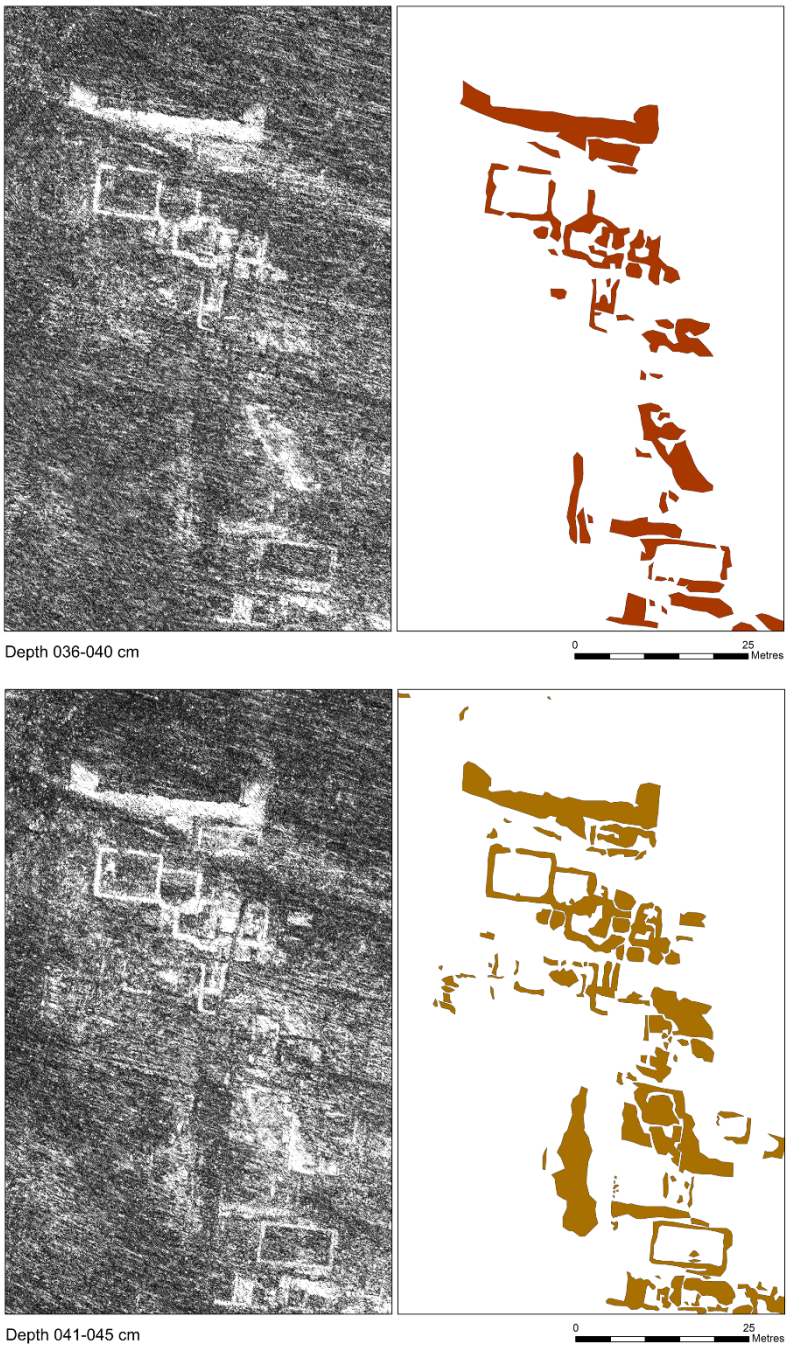

Figure S2. GPR time-slices from the sample area at Falerii Novi (for location see Figure 4) at depths 036–040cm and 041–045cm: left) GPR image; right) manually mapped anomalies (illustration: A. Launaro; GPR data: L. Verdonck).

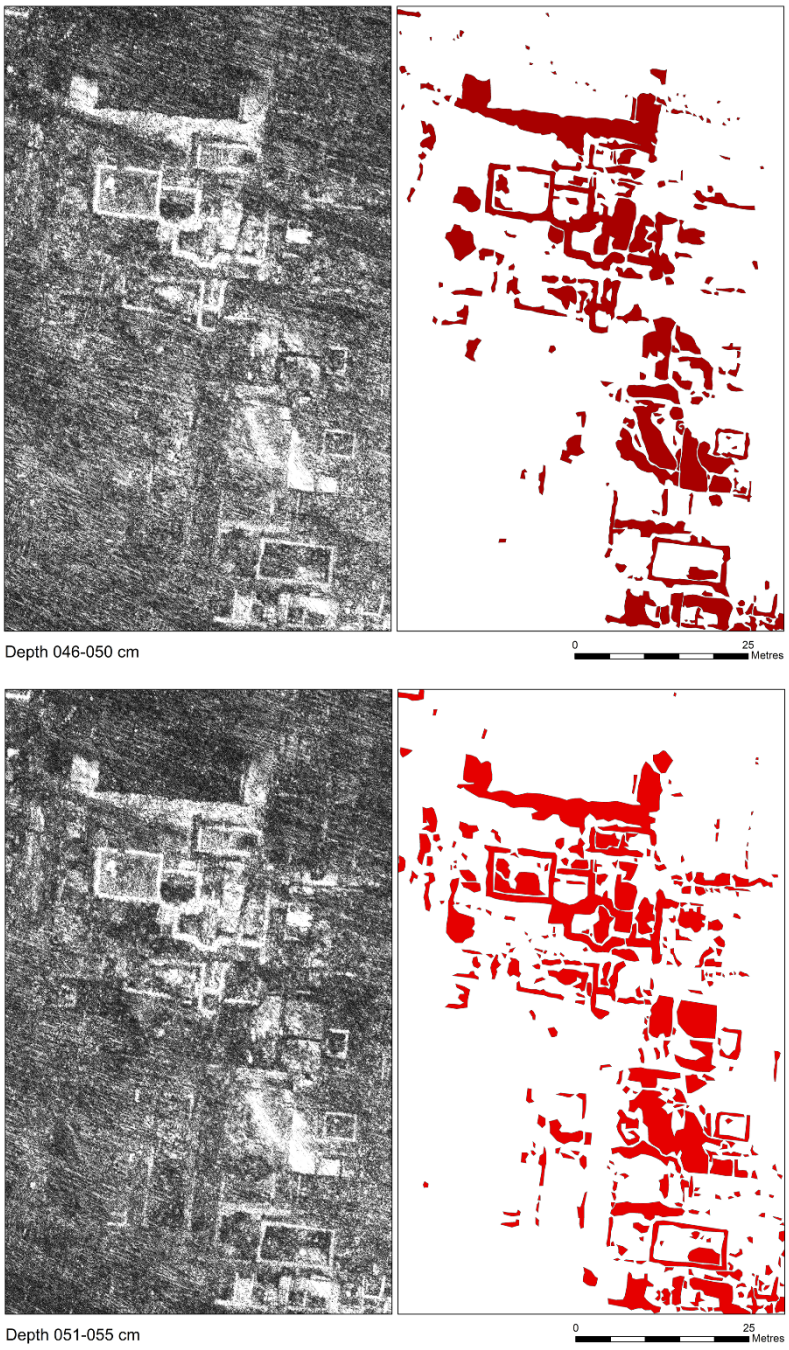

Figure S3. GPR time-slices from the sample area at Falerii Novi (for location see Figure 4) at depths 046–050cm and 051–055cm: left) GPR image; right) manually mapped anomalies (illustration: A. Launaro; GPR data: L. Verdonck).

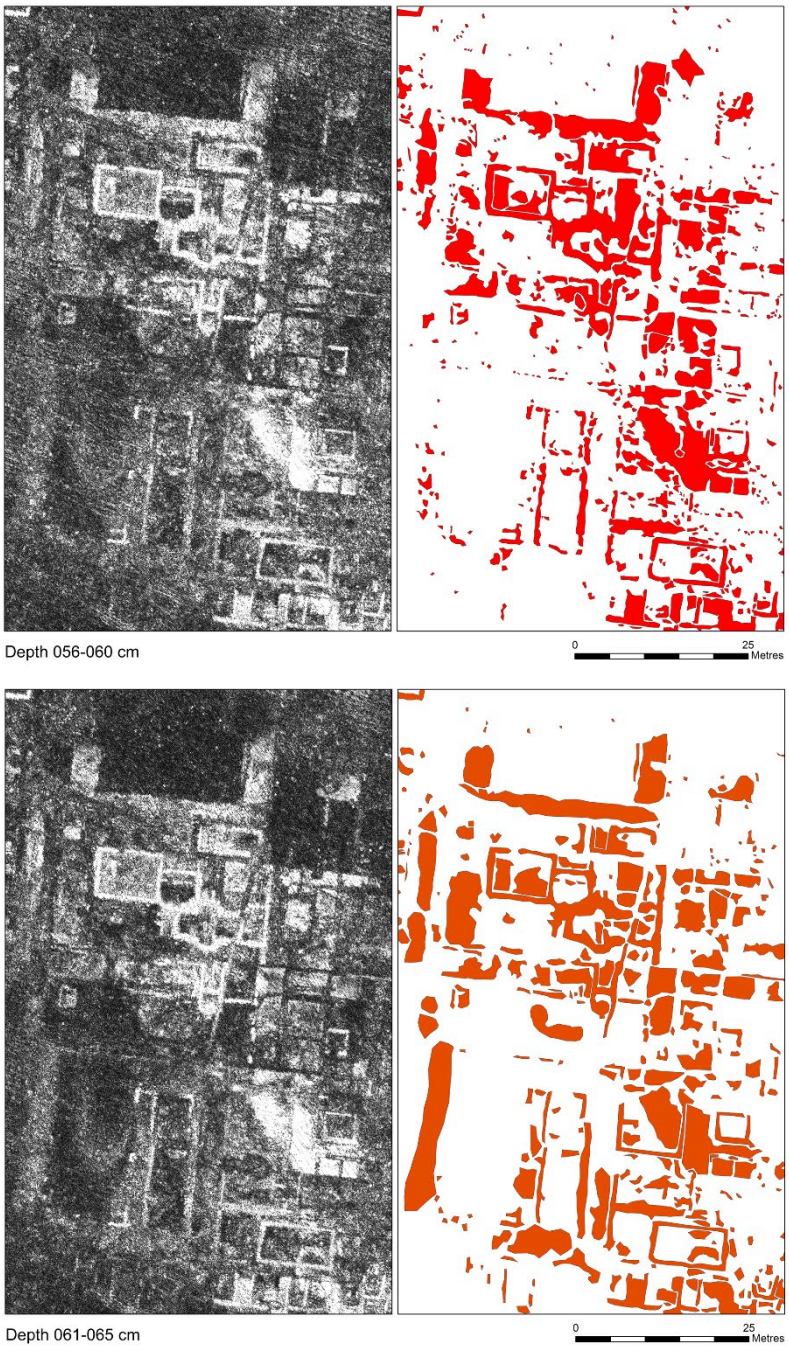

Figure S4. GPR time-slices from the sample area at Falerii Novi (for location see Figure 4) at depths 056–060cm and 061–065cm: left) GPR image; right) manually mapped anomalies (illustration: A. Launaro; GPR data: L. Verdonck).

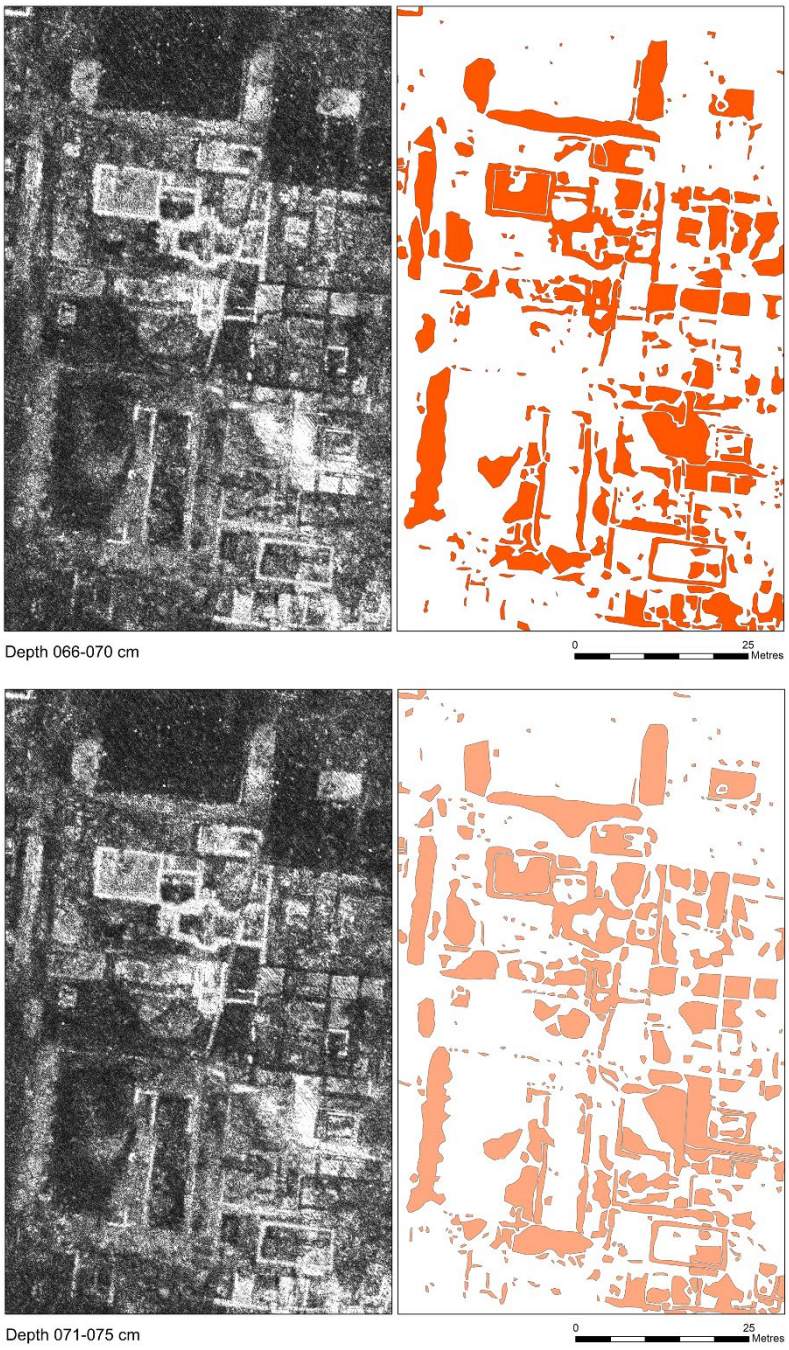

Figure S5. GPR time-slices from the sample area at Falerii Novi (for location see Figure 4) at depths 066–070cm and 071–075cm: left) GPR image; right) manually mapped anomalies (illustration: A. Launaro; GPR data: L. Verdonck).

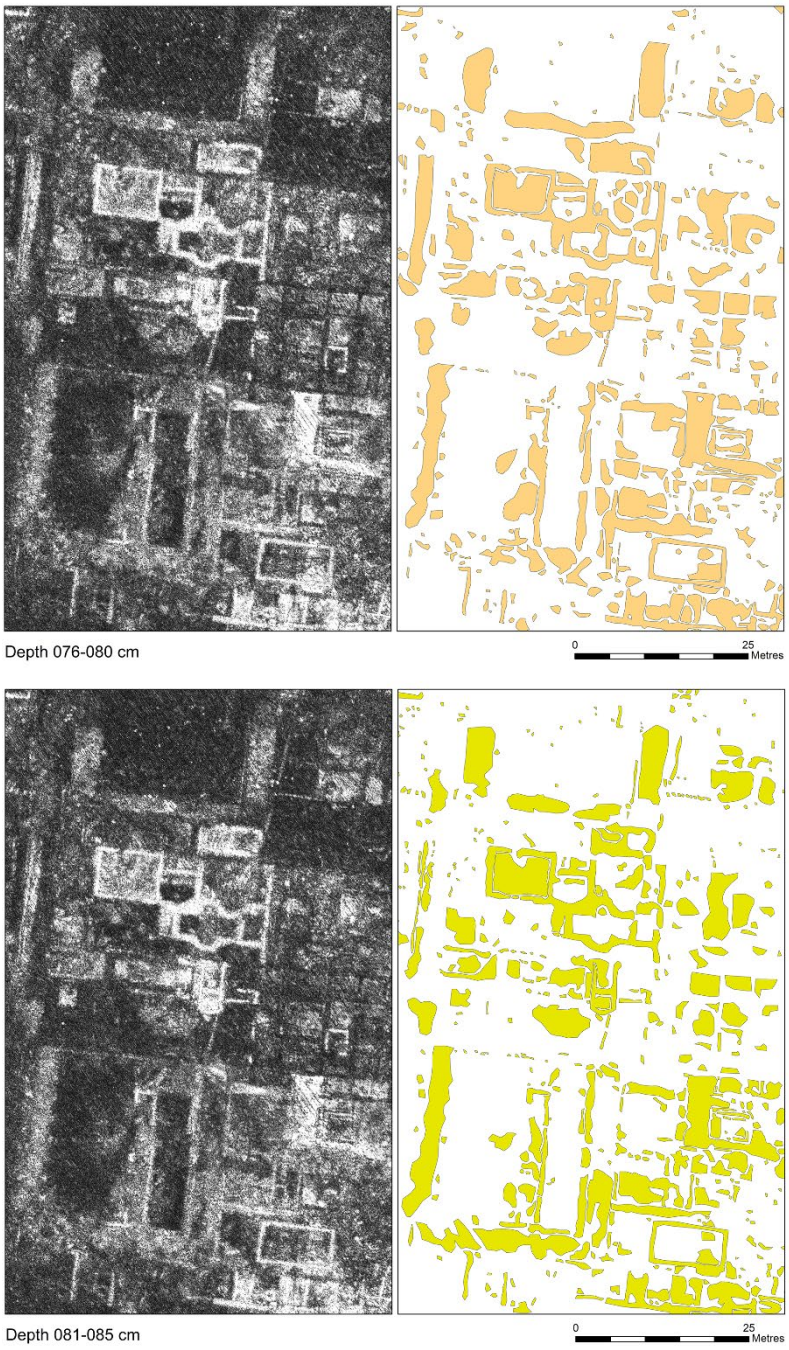

Figure S6. GPR time-slices from the sample area at Falerii Novi (for location see Figure 4) at depths 076–080cm and 081–085cm: left) GPR image; right) manually mapped anomalies (illustration: A. Launaro; GPR data: L. Verdonck).

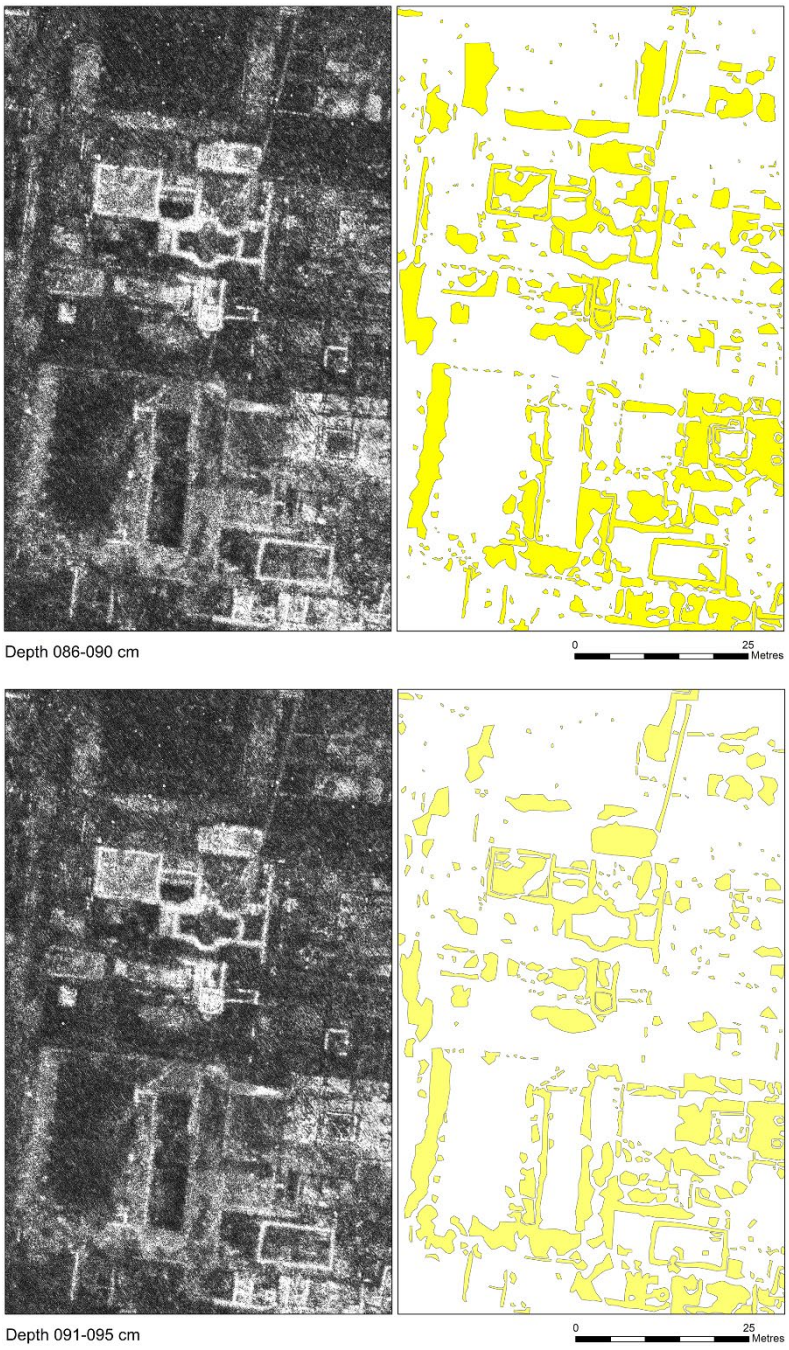

Figure S7. GPR time-slices from the sample area at Falerii Novi (for location see Figure 4) at depths 086–090cm and 091–095cm: left) GPR image; right) manually mapped anomalies (illustration: A. Launaro; GPR data: L. Verdonck).

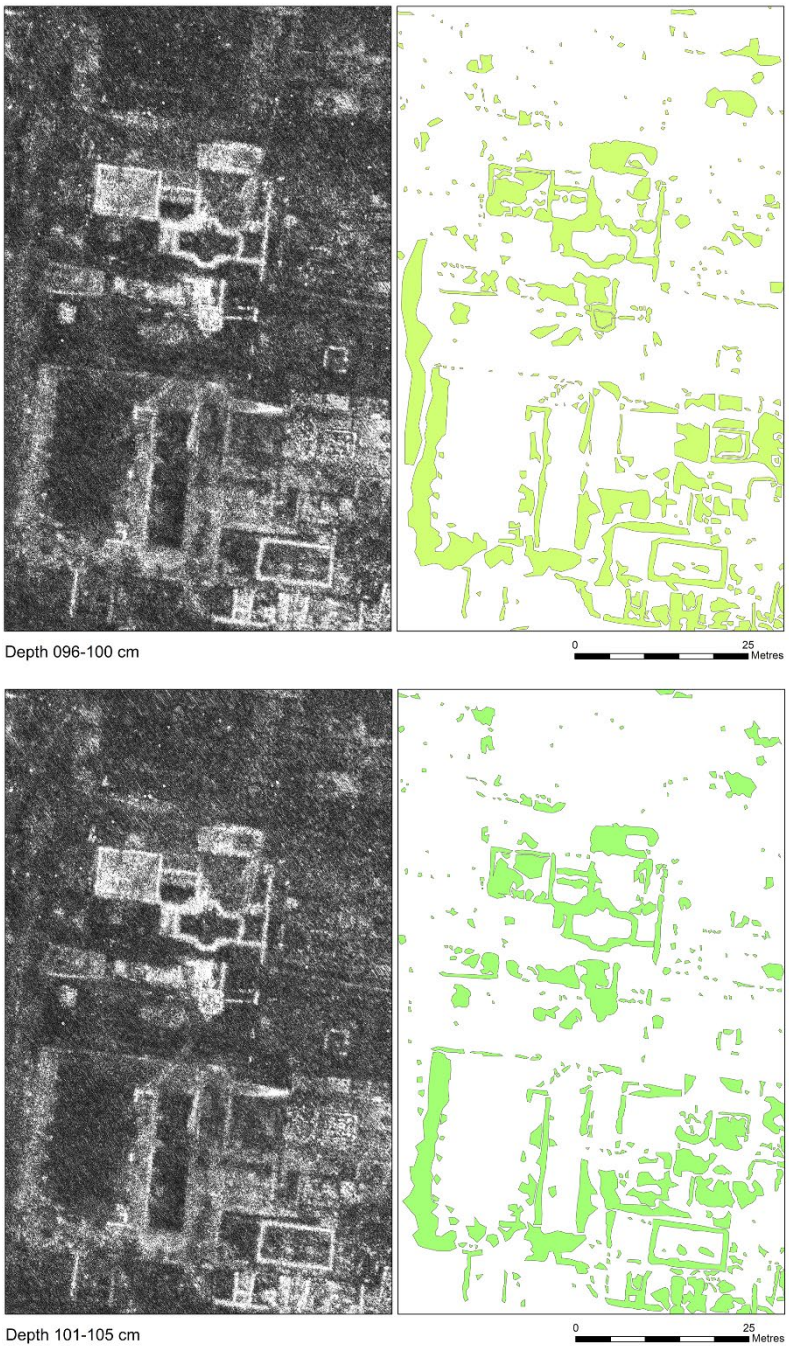

Figure S8. GPR time-slices from the sample area at Falerii Novi (for location see Figure 4) at depths 096–100cm and 101–105cm: left) GPR image; right) manually mapped anomalies (illustration: A. Launaro; GPR data: L. Verdonck).

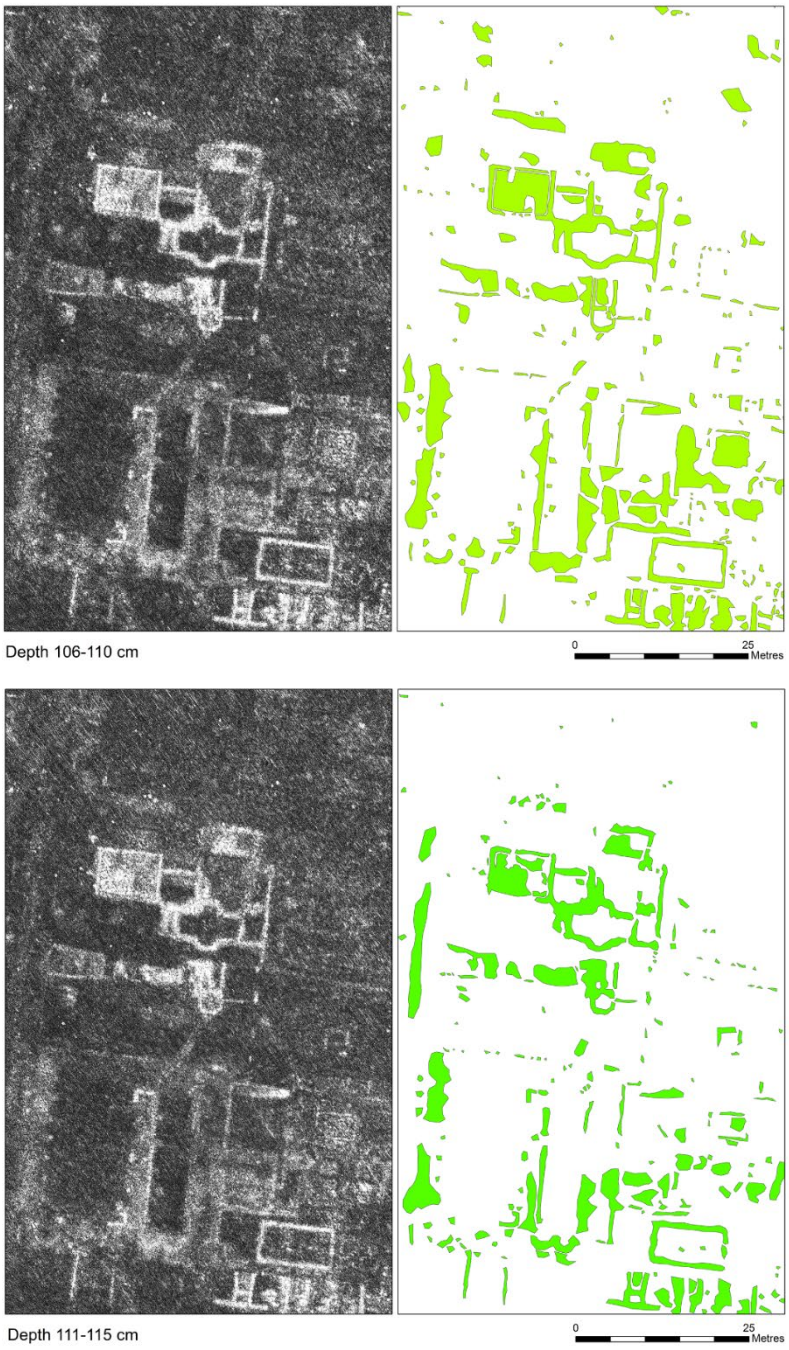

Figure S9. GPR time-slices from the sample area at Falerii Novi (for location see Figure 4) at depths 106–110cm and 111–115cm: left) GPR image; right) manually mapped anomalies (illustration: Al. Launaro; GPR data: L. Verdonck).

Figure S10. GPR time-slices from the sample area at Falerii Novi (for location see Figure 4) at depths 116–120cm and 121–125cm: left) GPR image; right) manually mapped anomalies (illustration: A. Launaro; GPR data: L. Verdonck).

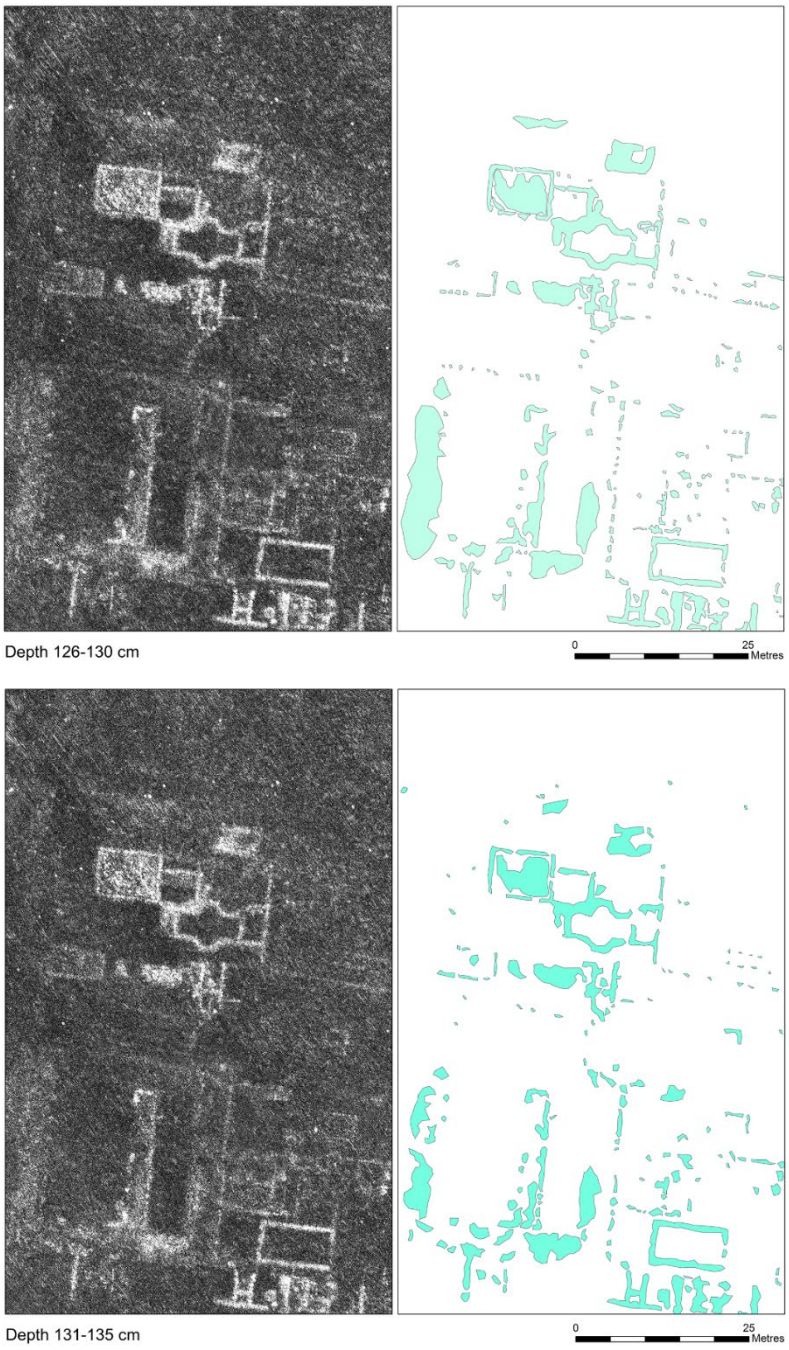

Figure S11. GPR time-slices from the sample area at Falerii Novi (for location see Figure 4) at depths 126–130cm and 131–135cm: left) GPR image; right) manually mapped anomalies (illustration: A. Launaro; GPR data: L. Verdonck).

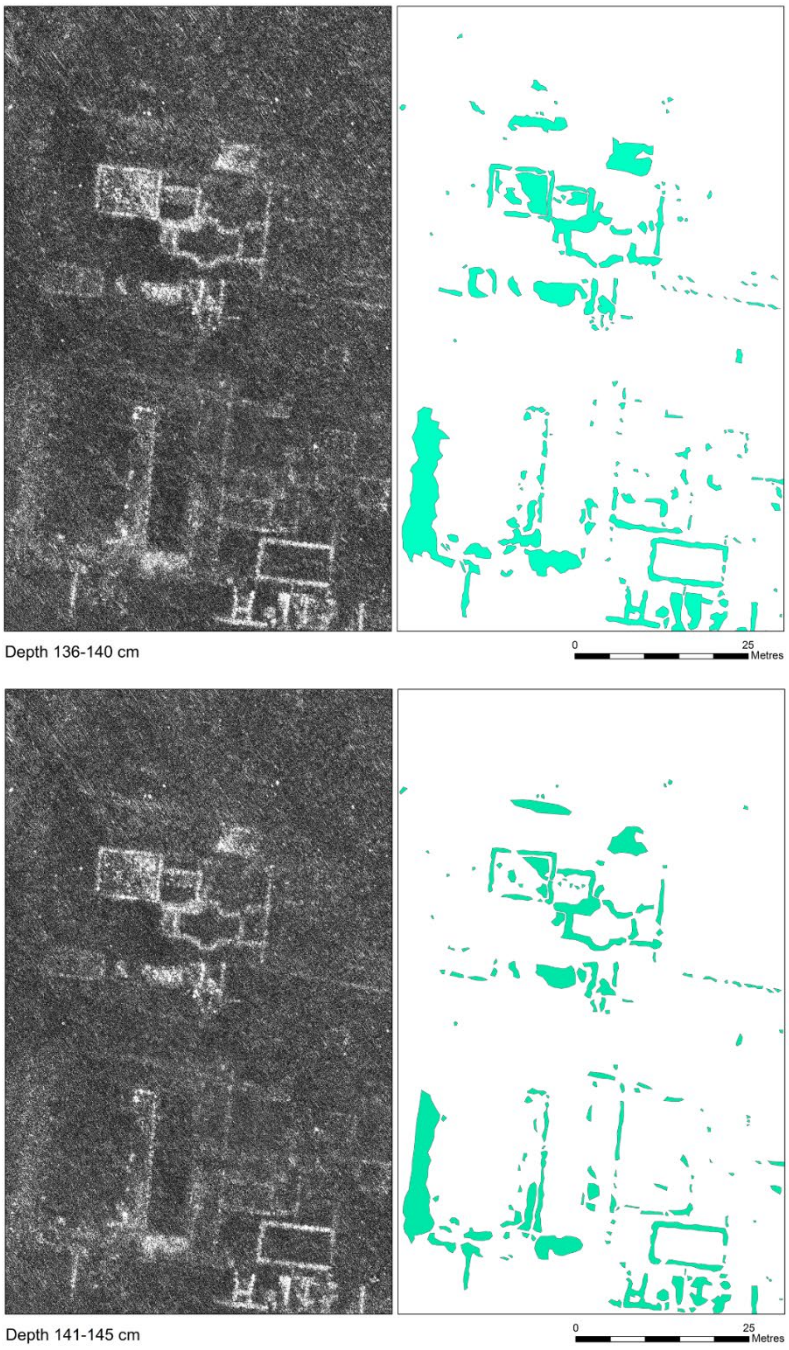

Figure S12. GPR time-slices from the sample area at Falerii Novi (for location see Figure 4) at depths 136–140cm and 141–145cm: left) GPR image; right) manually mapped anomalies (illustration: A. Launaro; GPR data: L. Verdonck).

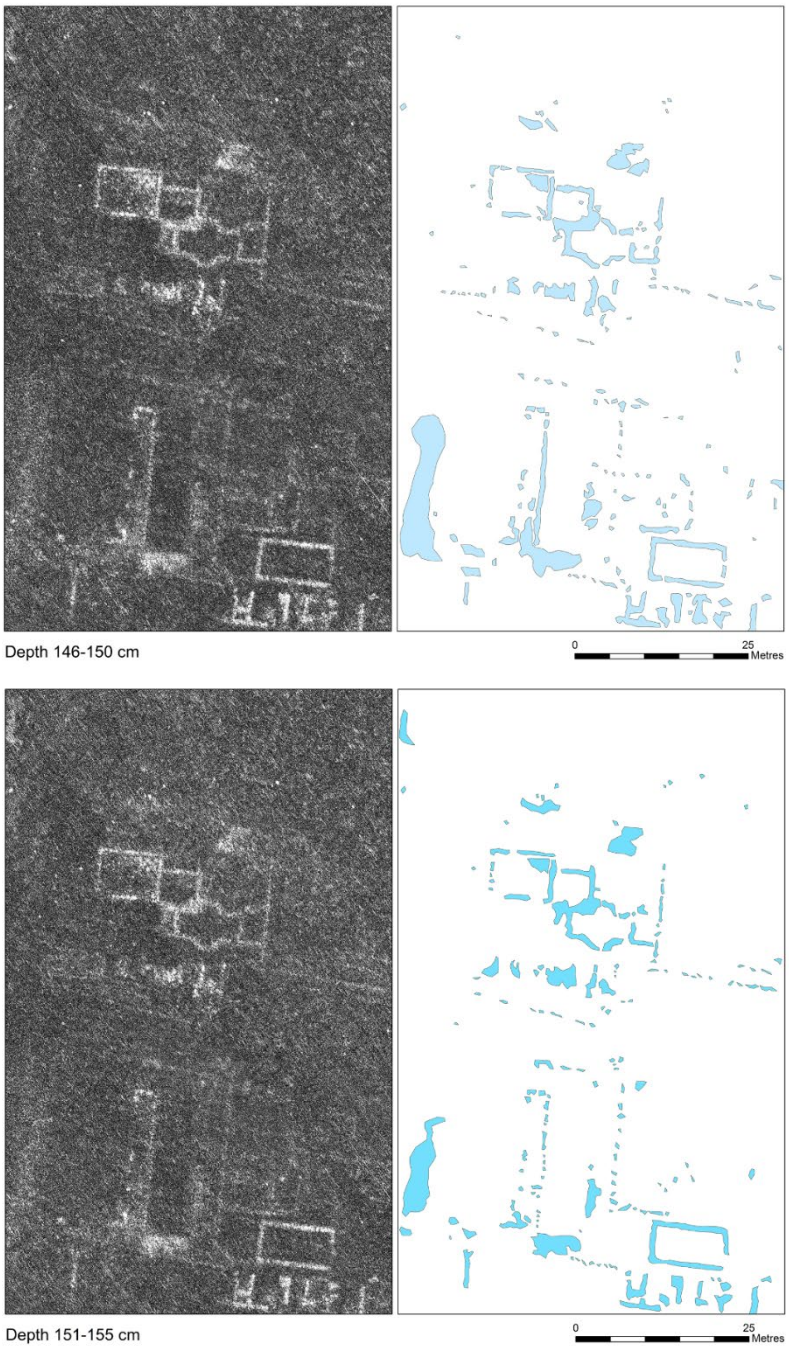

Figure S13. GPR time-slices from the sample area at Falerii Novi (for location see Figure 4) at depths 146–150cm and 151–155cm: left) GPR image; right) manually mapped anomalies (illustration: A. Launaro; GPR data: L. Verdonck).

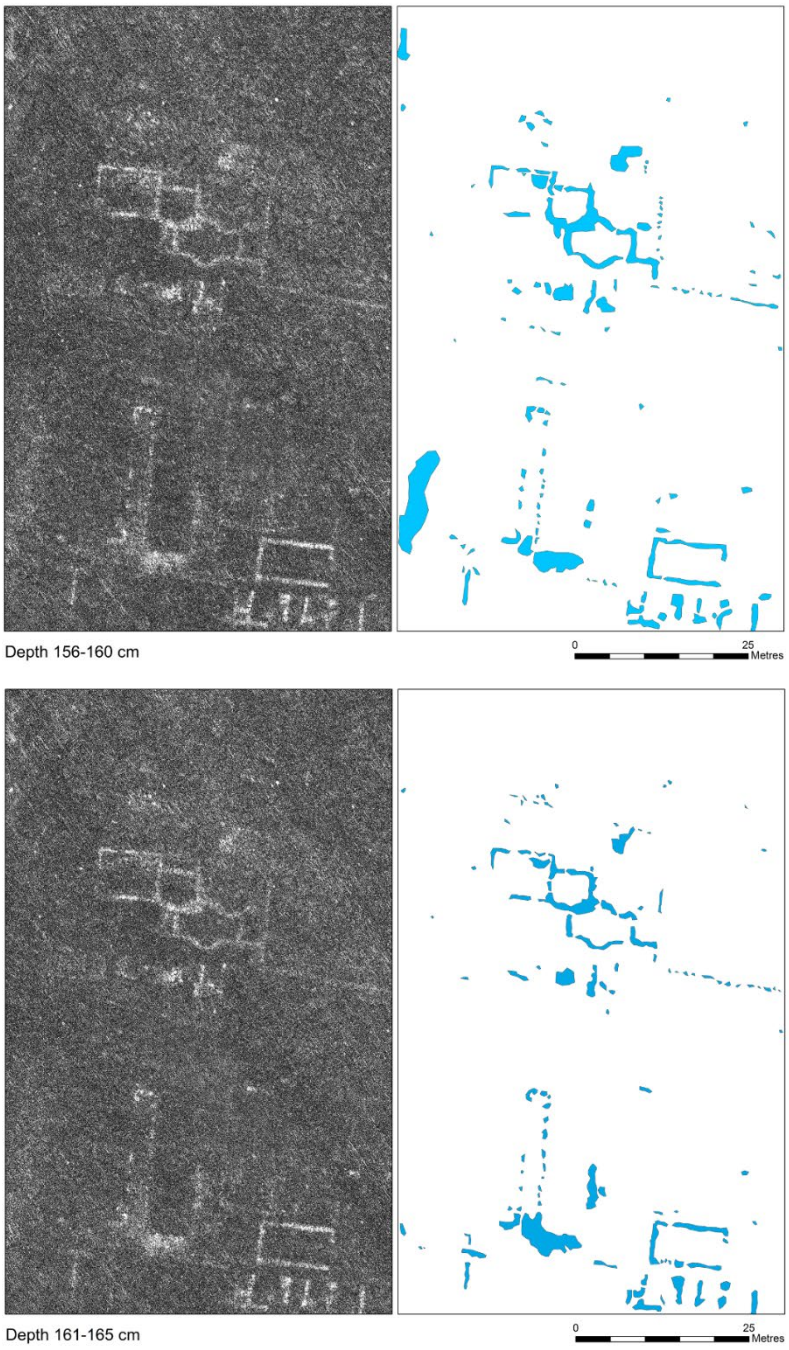

Figure S14. GPR time-slices from the sample area at Falerii Novi (for location see Figure 4) at depths 156–160cm and 161–165cm: left) GPR image; right) manually mapped anomalies (illustration: A. Launaro; GPR data: L. Verdonck).

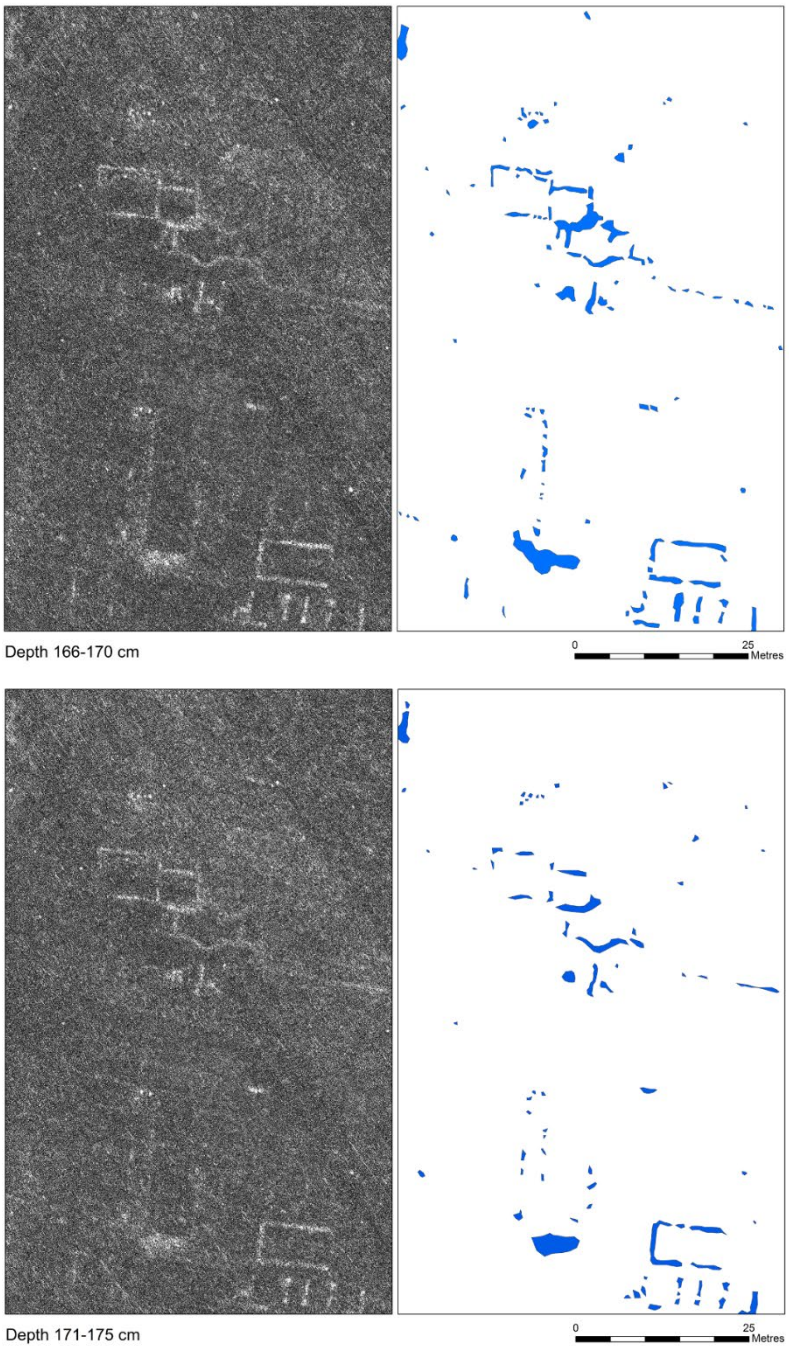

Figure S15. GPR time-slices from the sample area at Falerii Novi (for location see Figure 4) at depths 166–170cm and 171–175cm: left) GPR image; right) manually mapped anomalies (illustration: A. Launaro; GPR data: L. Verdonck).

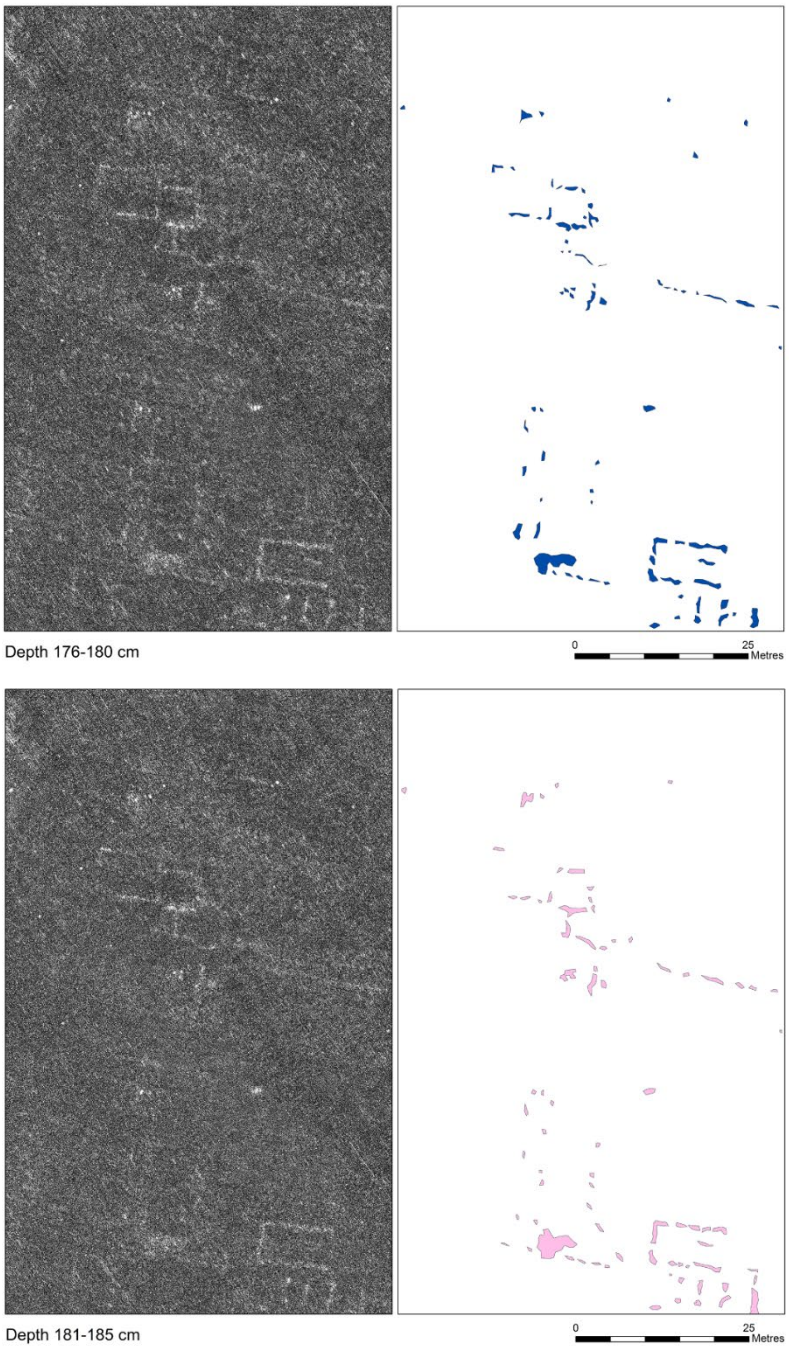

Figure S16. GPR time-slices from the sample area at Falerii Novi (for location see Figure 4) at depths 176–180cm and 181–185cm: left) GPR image; right) manually mapped anomalies (illustration: A. Launaro; GPR data: L. Verdonck).

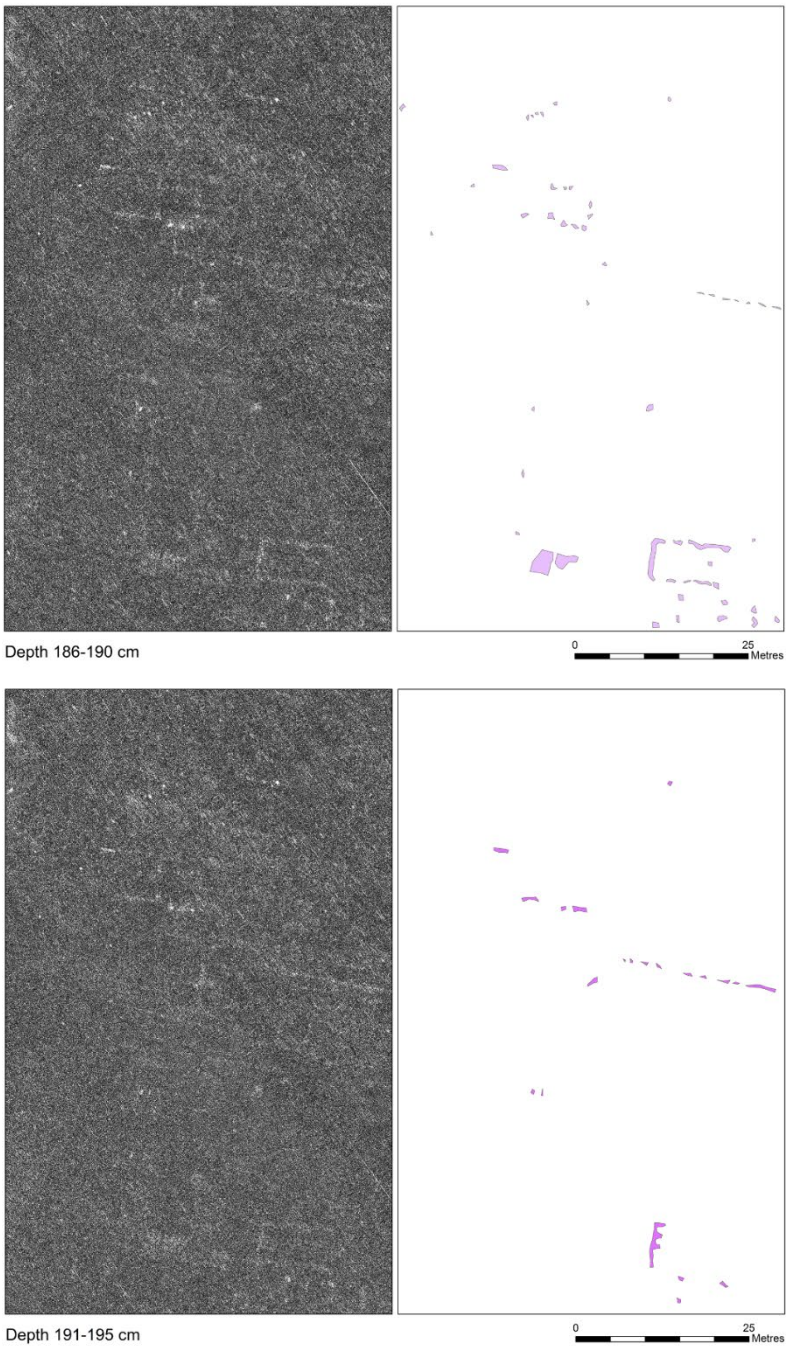

Figure S17. GPR time-slices from the sample area at Falerii Novi (for location see Figure 4) at depths 186–190cm and 191–195cm: left) GPR image; right) manually mapped anomalies (illustration: A. Launaro; GPR data: L. Verdonck).

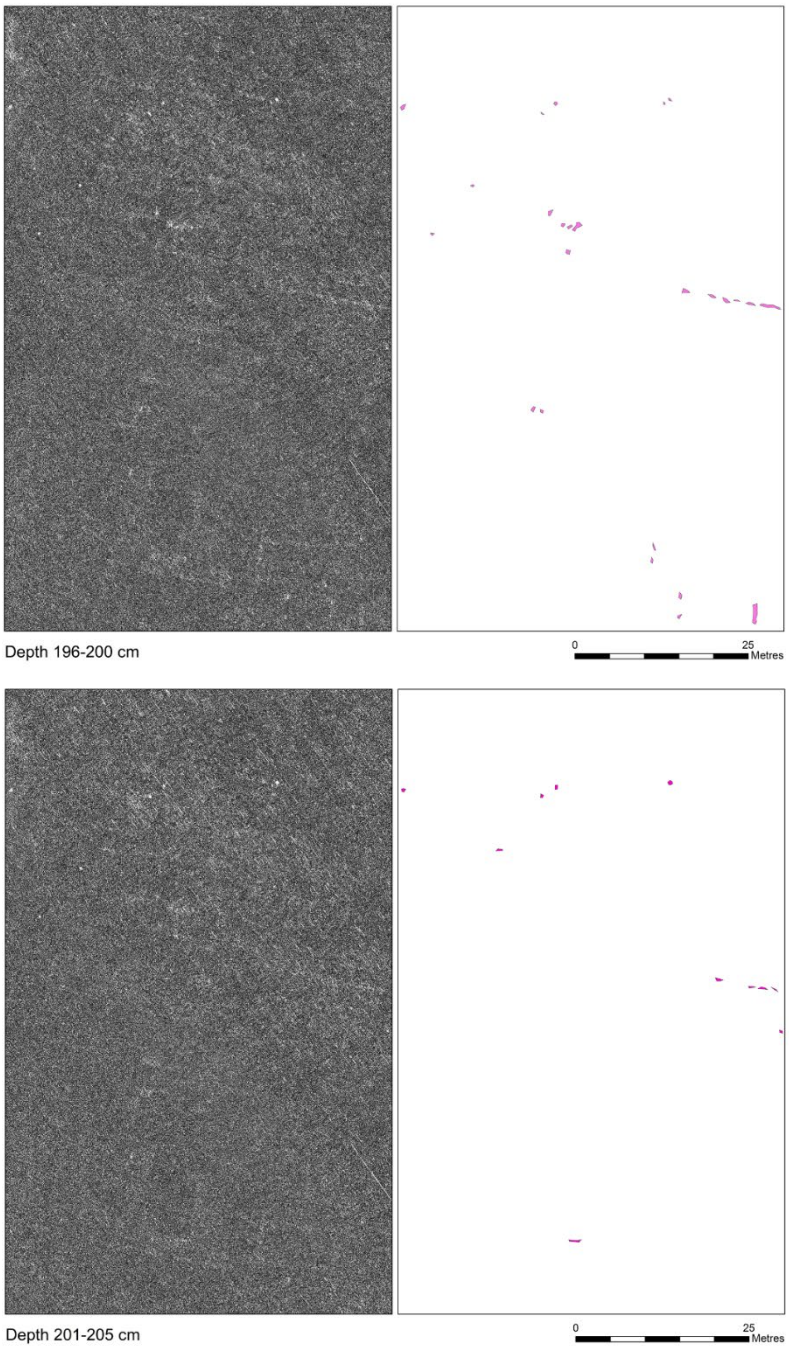

Figure S18. GPR time-slices from the sample area at Falerii Novi (for location see Figure 4) at depths 196–200cm and 201–205cm: left) GPR image; right) manually mapped anomalies (illustration: A. Launaro; GPR data: L. Verdonck).

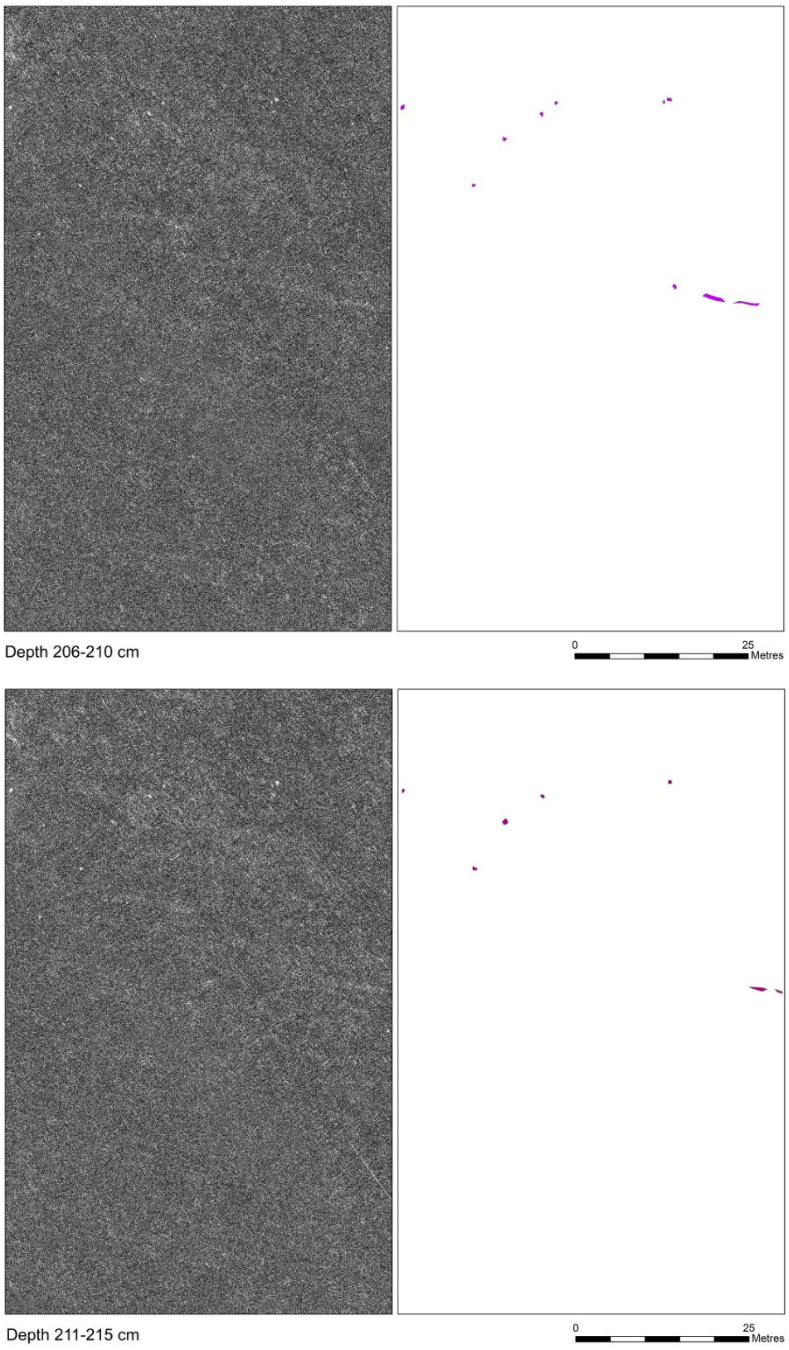

Figure S19. GPR time-slices from the sample area at Falerii Novi (for location see Figure 4) at depths 206–210cm and 211–215cm: left) GPR image; right) manually mapped anomalies (illustration: A. Launaro; GPR data: L. Verdonck).

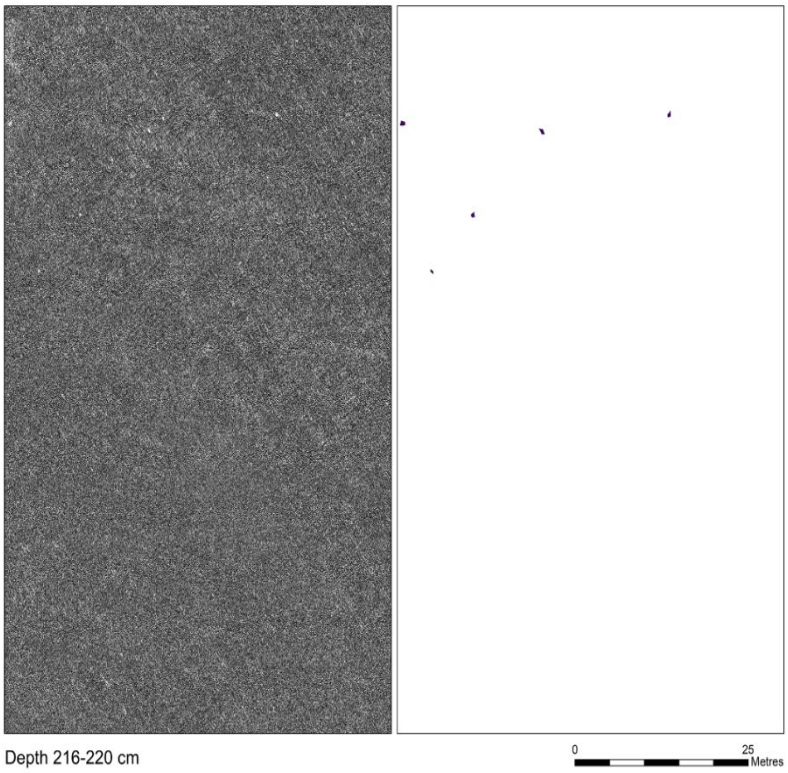

Figure S20. GPR time-slice from the sample area at Falerii Novi (for location see Figure 4) at depth 216–220cm: left) GPR image; right) manually mapped anomalies (illustration: A. Launaro; GPR data: L. Verdonck).